Axial Position Estimation through an Injection-based Self-sensing Technique for Hybrid Active-Passive Self-bearing Machines

1st Joachim Van Verdeghem
Mechatronic, Electrical Energy, and Dynamic Systems
Université catholique de Louvain (UCLouvain)
Louvain-La-Neuve, Belgium
joachim.vanverdeghem@uclouvain.be

2nd Bruno Dehez
Mechatronic, Electrical Energy, and Dynamic Systems
Université catholique de Louvain (UCLouvain)
Louvain-La-Neuve, Belgium
bruno.dehez@uclouvain.be

***Abstract*—Self-bearing machines are designed to be the centerpiece of highly integrated magnetically suspended systems by combining the rotor guidance and drive within a single structure. Their compactness and reliability have been taken a step further with the development of self-bearing machines that do not require sensors, controllers and power electronics to guide the rotor. In these passively levitated machines, the suspension of the axial degree of freedom relies on circulating currents that are induced in the armature windings thanks to the permanent magnet motion. The rotor can therefore not be axially stabilised at zero rotational speed. Hybrid actuation approaches, based on the active control of the rotor position until passive operation can be achieved, have been investigated. However, the requirement for a position sensor compromises the advantages of passive levitation. In this context, this paper proposes a self-sensing technique relying on the injection of a high frequency signal to estimate the winding impedance and extract the rotor axial position. Simulations of the rotor dynamics are performed on the basis of an electromechanical model of the machine to validate the operation principle, assess the tracking capabilities and investigate the robustness of this self-sensing technique.**

***Index Terms*—Bearingless machines, self-bearing motors, passive suspension, high frequency injection, sensorless**

I. Introduction

The development of self-bearing machines, that integrate the rotor guidance and drive into a single structure, has intensified in recent years due to the large demand for high power density magnetically suspended systems [1]. The five degrees of freedom of their rotor are typically stabilised by regulating the currents flowing in the windings of the machine according to position measurements. Despite the benefits in terms of rotor positioning and vibration management, the active control necessitates specific sensors, controllers and power electronics that affect the system cost, reliability and compactness in comparison with classic electrical machines equipped with ball bearings. One of the current challenge in the development of self-bearing machines is therefore to eliminate these elements by ensuring the rotor levitation through passive phenomena.

This work is funded by the Walloon Region (Belgium), SPW-Economie Emploi Recherche through the Win2Wal program, convention #2010131.

Electrodynamic forces arise from currents induced in windings due to their relative motion with respect to permanent magnets. Passively levitated self-bearing machines with combined windings based on this principle have recently been proposed [2, 3]. Their dynamic behaviour has been extensively studied theoretically through lumped-parameter electromechanical models and validated experimentally for both axial-flux [2] and radial-flux structures [3]. The impact of rotor ferromagnetic yokes placed behind the windings has been investigated via finite element model simulations [4] and analytically modelled [5], highlighting an improvement of the torque capability as well as additional force terms resulting from the variation of the inductance coefficients with the rotor axial position. Nevertheless, due to the passive mechanism at the origin of the force creation, the axial suspension can not be ensured at zero and even low spin speeds. To tackle this limitation, an hybrid actuation approach of these machines has been introduced and relies on the active control of the axial position until passive suspension forces are sufficient to support the rotor [6, 7]. The introduction of an external sensor, that would mitigate the advantages of passive levitation, can be avoided by implementing self-sensing techniques allowing the estimation of the rotor axial position.

Self-sensing techniques can be classified in two main categories. On the one hand, the rotor position can be retrieved at medium and high speeds from the back-electromotive forces (EMF), the latter being e.g. evaluated through state observers, such as Luenberger and sliding-mode observers [8], extended Kalman filter (EKF) or model reference adaptive system (MRAS) [9, 10], based on the fundamental-wave model of the machine. On the other hand, the estimation can be extracted from the variation of the winding inductance coefficients with the rotor position by superimposing a high frequency signal to the motor currents [11, 12]. Observer-based self-sensing techniques have already been derived for the hybrid active-passive self-bearing machine [13]. In contrast, although the rotor ferromagnetic yokes create an inductance variation, the injection-based technique has not been investigated yet.

In this context, this paper proposes and validates, through simulations performed in dynamic conditions, a self-sensing technique estimating the rotor axial position at zero and very low speeds on the basis of the winding synchronous inductance coefficients by injecting a high frequency signal and analysing the resulting current variation.

The paper is structured as follows. Section II first describes the structure and the operation principle of the self-bearing machine and then derives the electromechanical model predicting the rotor axial and spin dynamics. Following on from this, Section III presents a high frequency signal injection self-sensing technique allowing to estimate the rotor axial displacement based on the position-related inductance variation. Finally, the operation and the robustness of the proposed technique are investigated through dynamic simulations carried out in the framework of a case study in Section IV.

II. Machine Description

This section first presents the structure and the operation principle of the self-bearing machine. The electromechanical model predicting the rotor axial and spin dynamics in active suspension mode is then established.

A. Structure & Principle

The structure of the self-bearing machine under study is represented in Fig. 1(a). The rotor consists of permanent magnets producing an axial magnetic field with p pole pairs and ferromagnetic yokes fixed on both sides of the latter. This configuration allows to enclose the magnetic field within the machine while preventing a negative magnetic stiffness arising from the attraction forces between the permanent magnets and the ferromagnetic parts. The stator encompasses two three-phase windings located in the airgaps between the rotor permanent magnets and the yokes. Their connection to the power supply varies according to the hybrid active-passive operating mode of the axial suspension [6].

In passive suspension mode, the motor current i_M provided by the power supply flows through both windings connected in parallel, creating only a drive torque as in a conventional electrical machine. When the rotor leaves its centred position ($z \neq 0$), circulating suspension currents i_S, adding to the classic motor current i_M, are induced due to an unbalance between the upper and lower winding flux linkages and generate an axial restoring force as well as an undesirable drag torque, as depicted in Fig. 1(b). The force creation resulting from induced currents, passive rotor levitation can not be achieved at zero and low speeds. Active control of the rotor position is therefore implemented in this speed region.

In active suspension mode, one three-phase winding is connected to the power supply while the second is left open, as shown in Fig. 1(c). The resulting asymmetric structure is identical to the single-drive self-bearing motor investigated in [14]. The axial force and the drive torque can then be regulated, regardless of the rotational speed ω, through the direct and quadrature components of the motor current i_M respectively. This active control requires the rotor axial position

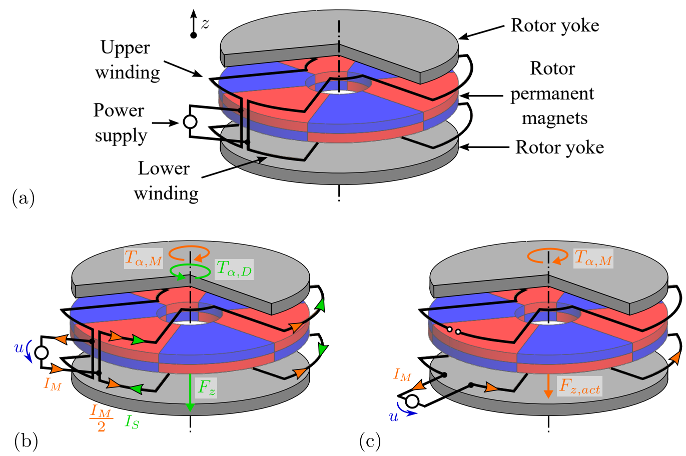

Fig. 1: Self-bearing machine (only one phase represented with $p = 3$). (a) Structure. (b) Passive suspension operation at high speeds. (c) Active suspension operation at low speeds.

information. To prevent the addition of a dedicated sensor that would jeopardise the benefits of passive levitation, the axial position z can be estimated through self-sensing techniques, either based on state observers [13] or high frequency signal injection, as described hereinafter.

B. Electromechanical Model

Under the assumption of small rotor displacements, the winding synchronous inductance coefficient L_c is supposed to evolve linearly with the axial position z:

$$L_c = L_{0,c} + zL_{z,c} \tag{1}$$

where $L_{0,c}$ is the synchronous inductance coefficient in centred position and $L_{z,c}$ is the synchronous variational inductance coefficient, i.e. the proportionality factor between the inductance and the rotor axial position z. On this basis and following an approach identical to that adopted in [5] for the passive operation, the electromechanical model governing the rotor dynamics in active suspension mode can be expressed as:

$$\begin{aligned}
u_d &= (R + \dot{z}L_{z,c})\, i_{M,d} + \dot{z}K_z\sqrt{\frac{3}{2}} \\
&\quad + (L_{0,c} + zL_{z,c})[\dot{i_{M,d}} - p\omega i_{M,q}] \\
u_q &= (R + \dot{z}L_{z,c})\, i_{M,q} + p\omega(K_\alpha + zK_z)\sqrt{\frac{3}{2}} \\
&\quad + (L_{0,c} + zL_{z,c})[\dot{i_{M,q}} + p\omega i_{M,d}] \\
m\ddot{z} &= K_z\sqrt{\frac{3}{2}}i_{M,d} + \frac{L_{z,c}}{2}(i_{M,d}^2 + i_{M,q}^2) - C_z\dot{z} + F_e \\
J_p\dot{\omega} &= p(K_\alpha + zK_z)\sqrt{\frac{3}{2}}i_{M,q} + T_e
\end{aligned} \tag{2}$$

where u_d and u_q are the direct and quadrature-axis components of the voltage supplied to the armature, R is the winding resistance, K_α is the flux constant, namely the amplitude of the permanent magnet flux linked by the windings in centred position, K_z is the flux gradient, i.e. the proportionality factor

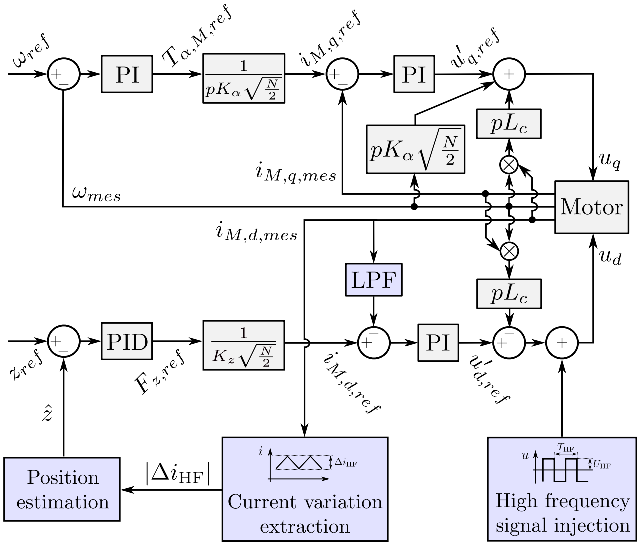

Fig. 2: Control block diagram including the injection-based self-sensing technique (highlighted in blue).

between the variation of amplitude of the PM flux linkage and the axial position, m and J_p are the rotor mass and polar moment of inertia, C_z is the axial external damping, F_e and T_e are the load force and torque applied on the rotor.

The machine electrical equations show that the rotor axial position information is contained in the terms linked to the synchronous inductance coefficient, exploitable at zero and low speeds as further developed in Section III, as well as in the back-electromotive force, exploitable at medium and high speeds through state observers as described in [13].

III. Self-sensing Technique

The proposed self-sensing technique aims at estimating the rotor axial displacement z at zero and low rotational speed ω by evaluating the inductance coefficients, the latter varying with the position thanks to the ferromagnetic yokes placed behind the windings. To that end, a high frequency signal is superimposed to the voltage provided by the current controller and the resulting high frequency variation of the measured currents is extracted and analysed, as represented in Fig. 2 and detailed hereinafter.

A. High Frequency Injection

The injection scheme is implemented in the Park reference frame and leans on a pulsating square-wave signal, thus allowing to use higher frequency compared to conventional sinusoidal injection. The electrical model (2) can be simplified assuming that the terms linked to the rotational speed ω are negligible, the latter being low and much lower than the frequency of the injected signal:

$$\begin{aligned} u_d &= (R + \dot{z}L_{z,c})\, i_{M,d} + (L_{0,c} + zL_{z,c})\dot{i}_{M,d} + \dot{z}K_z\sqrt{\tfrac{3}{2}} \\ u_q &= (R + \dot{z}L_{z,c})\, i_{M,q} + (L_{0,c} + zL_{z,c})\dot{i}_{M,q} \end{aligned} \tag{3}$$

The terms related to the rotor axial speed $\dot{z}$ can also be neglected, reducing the model to that of a classical R-L load for both direct and quadrature axes:

$$\begin{aligned} u_{d,\mathrm{HF}} &= R\, i_{M,d,\mathrm{HF}} + (L_{0,c} + zL_{z,c})\dot{i}_{M,d,\mathrm{HF}} \\ u_{q,\mathrm{HF}} &= R\, i_{M,q,\mathrm{HF}} + (L_{0,c} + zL_{z,c})\dot{i}_{M,q,\mathrm{HF}} \end{aligned} \tag{4}$$

These equations further simplifies assuming that the windings show an inductive behaviour at the injection frequency:

$$\begin{aligned} u_{d,\mathrm{HF}} &= (L_{0,c} + zL_{z,c})\dot{i}_{M,d,\mathrm{HF}} \\ u_{q,\mathrm{HF}} &= (L_{0,c} + zL_{z,c})\dot{i}_{M,q,\mathrm{HF}} \end{aligned} \tag{5}$$

However, due to the low inductance coefficients resulting from the slotless structure of the machine under study, this hypothesis is not necessarily verified.

In both cases, the signal injection can be performed on either axis given that the two electrical equations are identical. The amplitude of the high frequency currents is modulated by the rotor axial position z due to the inductance variation and so are the resulting upper and lower envelopes of the total motor current, that includes the conventional current at the origin of the force and torque creation.

B. Current Variation Extraction

The proposed self-sensing technique relies on a square-wave signal and therefore do not require filters for the demodulation of the high frequency current variation, unlike conventional sinusoidal voltage injection, thereby preventing the underlying phase lags. Specifically, the high frequency currents feature the classical negative exponential time response of a R-L circuit subjected to a voltage step. The resulting current variation Δi_{HF}, that corresponds to the difference between the upper and lower envelopes of the total current, can therefore be easily extracted during the machine operation by subtracting the currents measured at the beginning of two successive half period of injection, as represented in Fig. 3. On the other hand, considering a symmetrical square-wave signal with an amplitude U_{HF} and a period T_{HF}, the theoretical expression of the high frequency current variation Δi_{HF} can be calculated based on (4), yielding:

$$\Delta i_{\mathrm{HF}}(z) = \pm\frac{2U_{\mathrm{HF}}}{R}\left(\frac{\exp\left(\frac{T_{\mathrm{HF}}}{2}\frac{R}{L_c(z)}\right) - 1}{\exp\left(\frac{T_{\mathrm{HF}}}{2}\frac{R}{L_c(z)}\right) + 1}\right). \tag{6}$$

Assuming that the winding resistance R is negligible compared to its reactance at the injection frequency, the currents evolve linearly with time and (6) reduces to:

$$\Delta i_{\mathrm{HF}}(z) = \pm\frac{U_{\mathrm{HF}}}{L_c(z)}\frac{T_{\mathrm{HF}}}{2}. \tag{7}$$

The current variation Δi_{HF} thus depends, in addition to the synchronous inductance coefficient L_c as required for the position estimation, solely on the characteristics of the injected signal U_{HF} and T_{HF}. This prevents errors arising from uncertainties on the electrical winding resistance R, e.g. due to the effect of temperature.

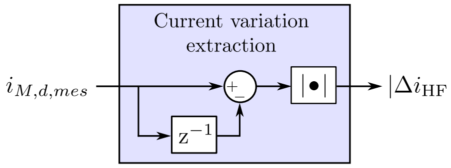

Fig. 3: Block diagram of the extraction of the high frequency current variation $|\Delta i_{\mathrm{HF}}|$ from the measured d-axis current.

C. Position Estimation

In the general case, an estimate of the synchronous inductance coefficient $\hat{L}_c$ can be obtained based on the absolute value of the high frequency current variation of the measured motor current Δi_{HF} and (6), yielding:

$$\hat{L}_c = \frac{R}{\log\left(\frac{2U_{\mathrm{HF}}+|\Delta i_{\mathrm{HF}}|R}{2U_{\mathrm{HF}}-|\Delta i_{\mathrm{HF}}|R}\right)} \frac{T_{\mathrm{HF}}}{2}. \tag{8}$$

This expression simplifies when the electrical resistance R has a negligible impact on the winding impedance:

$$\hat{L}_c = \frac{U_{\mathrm{HF}}}{|\Delta i_{\mathrm{HF}}|} \frac{T_{\mathrm{HF}}}{2}. \tag{9}$$

The rotor axial displacement z can finally be estimated by inverting the linear expression (1) that describes the evolution of the armature winding synchronous inductance coefficient L_c with the position:

$$\hat{z} = \frac{\hat{L}_c - L_{0,c}}{L_{z,c}} \tag{10}$$

It is important to note that, unlike self-sensing techniques developed to estimate the rotor spin position in conventional electric machines, the proposed method evaluates the axial displacement based on the inductance coefficient value itself. A precise knowledge of the winding impedance parameters is therefore required to provide an accurate position estimate.

D. Low-pass Filter

The self-sensing technique relies on the proper evaluation of the high frequency current variation Δi_{HF} resulting from the square-wave injected signal so as to retrieve the synchronous inductance coefficient L_c and, on this basis, estimate the axial position z. This method thus requires the excitation signal to be perfectly determined, implying that the output of the current controller should not include any high frequency component that would compromise the current response. Hence, depending on the closed-loop bandwidth of the current loop, selected based on the desired motor performance, and the injection frequency, a low-pass filter might be added on the direct-axis current feedback term to reject the high frequency component arising from the injected signal.

IV. Case Study

This section first aims to validate the operation principle of the proposed signal injection technique. Its robustness to errors on the machine parameters is then analysed. To that end, dynamic simulations are carried out on MATLAB SIMULINK on the basis of the electromechanical model (2).

TABLE I: Case study – Machine parameters

Symbol	Unit	Value
p	–	9
R	mΩ	159
L_c	μH	10.8
$L_{z,c}$	μH/mm	1.95
K_α	Wb	5.5
K_z	Wb/m	1.01
C_z	Ns/m	0
m	kg	0.5
J_p	gm^2	0.94

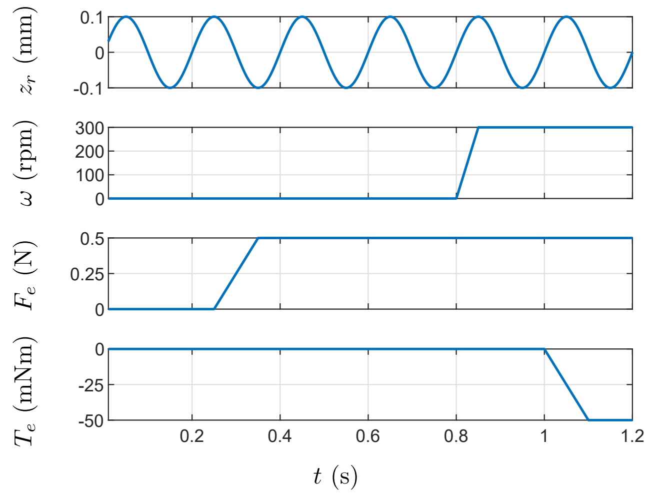

Fig. 4: Case study – Time evolution of the position setpoint z_r, rotor spin speed ω, axial external force F_e and load torque T_e throughout the sequence.

The high frequency signal is injected at 40 (kHz) on the direct axis with an amplitude of 125 (mV). The bandwidths of the closed-loop position and current controllers are set to 0.250 and 3 (kHz). The low-pass filter relies on two cascaded second order filters whose cut-off frequency is fixed to 8 (kHz). The machine parameters are listed in Table I.

A. Principle Validation

The self-sensing technique operation principle and tracking capabilities are assessed based on a specific sequence, described in Fig. 4. A sinusoidal rotor axial position setpoint with an amplitude of 0.1 (mm) and a frequency of 5 (Hz) is imposed. The spin speed reference is initially fixed at 0 (rpm) and then increases at 0.8 (s) to reach 300 (rpm) in 0.05 (s). The axial external force F_e exerted on the rotor gradually intensifies from 0.25 to 0.35 (s) up to 0.5 (N). Lastly, a load torque amounting to 50 (mNm) is applied at 1 (s).

Figs. 5(a) and 5(b) represent the time evolution of the high frequency injected signal, the output of the direct-axis current controller and the resulting voltage u_d applied to the self-bearing motor throughout the complete sequence and a focus

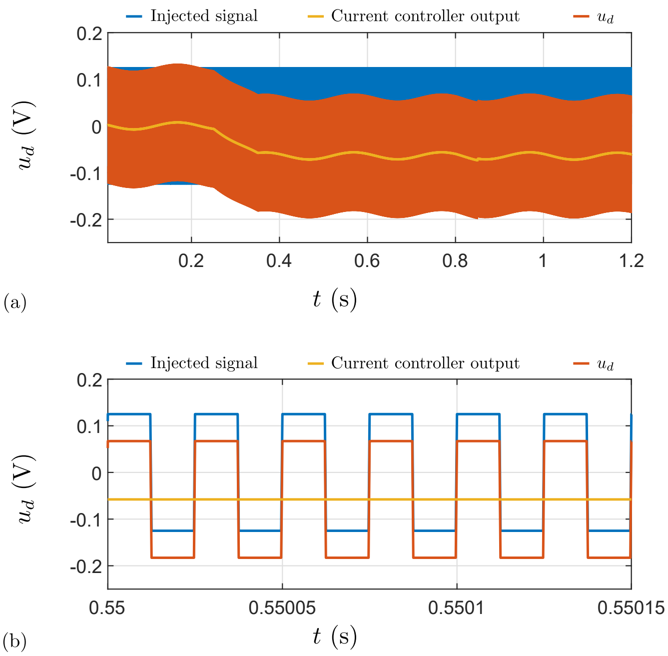

Fig. 5: Case study – Time evolution of the injected signal, the current controller output and the direct-axis voltage u_d applied to the self-bearing motor. (a) Complete sequence. (b) Focus on the high frequency signals.

on six injection periods respectively. As desired, the controller output show no high frequency component, implying that the current regulation does not interfere with the signal injection thanks to properly set bandwidths for the low-pass filter as well as the closed-loop position and current transfer functions.

Figs. 6(a) and 6(b) depict the time evolution of the actual and filtered d-axis current $i_{M,d}$. On the one hand, it can be observed that the low-pass filter bandwidth is indeed properly selected, the output solely evolving in accordance with the sinusoidal position setpoint and the variation of the external force F_e. On the other hand, the high frequency component of the current features the expected exponential time response of a R-L circuit and oscillates between an upper and a lower envelope. The absolute value of the high frequency current variation Δi_{HF}, that corresponds to the difference between these two envelopes, is illustrated in Fig. 6(c). Sinusoidal fluctuations that reflect the variation of the inductance coefficients due to rotor axial displacements are highlighted.

The synchronous inductance coefficient L_c can then be estimated by substituting the high frequency current amplitude Δi_{HF} extracted from the d-axis current into (8) as well as into the simplified variant (9), as shown in Fig. 7. As expected, the inductance coefficient varies around its centred value $L_{0,c}$, even though the deviations are rather low. Furthermore, the electrical resistance R amounts to 6% of the winding impedance at the injection frequency and is therefore not negligible, leading to an offset on the inductance estimate $\hat{L}_c$ that relies on the simplified equations.

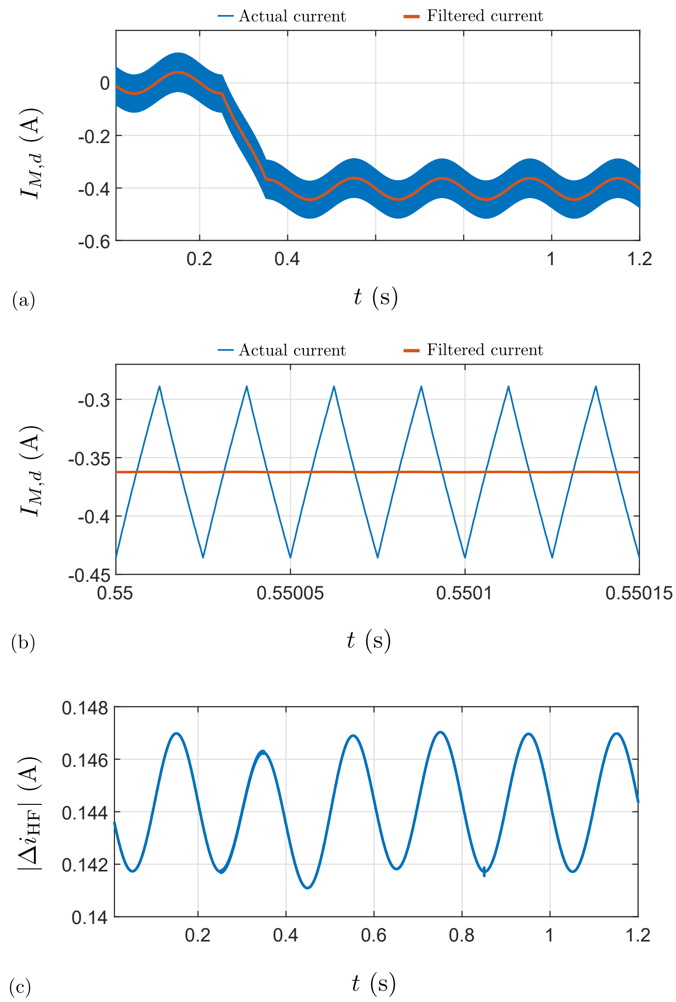

Fig. 6: Case study – Time evolution of the direct-axis motor current $i_{M,d}$. (a) Complete sequence. (b) Focus on the high frequency signals. (c) Absolute value of the high frequency current variation Δi_{HF}.

The rotor axial position z and its estimates $\hat{z}$, calculated through (10) on the basis of the estimated inductance coefficients $\hat{L}_c$, are presented in Fig. 8. The close agreement between the actual rotor displacement and the estimate based on the complete impedance validates the operation principle of the proposed self-sensing technique as well as its tracking capabilities in case of variable position setpoint, modification of the spin speed reference and step of axial external force. Finally, regarding the estimate that neglects the electrical resistance R, the shift error in the inductance $\hat{L}_c$ translates into an offset in the estimated rotor axial position $\hat{z}$. This simplified estimate is nonetheless of interest since the offset can be considered reasonable given that the machine could experience larger position deviation in passive suspension mode.

B. Robustness Analysis

The robustness of the self-sensing technique is investigated by studying the influence on the position estimate $\hat{z}$ of ±5%

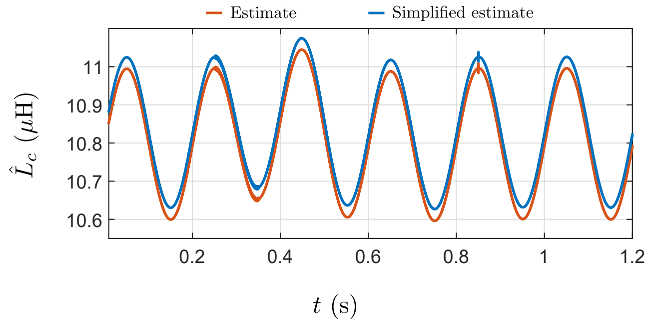

Fig. 7: Case study – Time evolution of the synchronous inductance coefficient estimates $\hat{L}_c$ based on the complete and simplified models, (8) and (9) respectively.

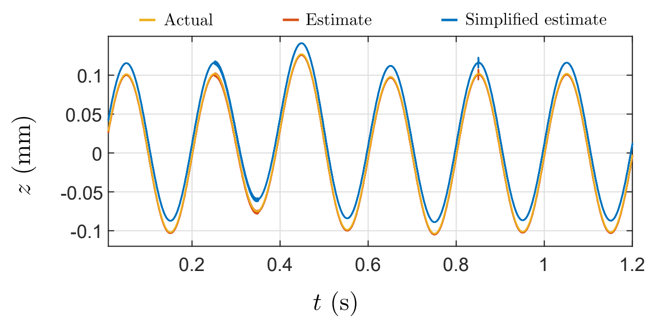

Fig. 8: Case study – Time evolution of the actual rotor axial position z and the estimates $\hat{z}$ based on the complete and simplified models.

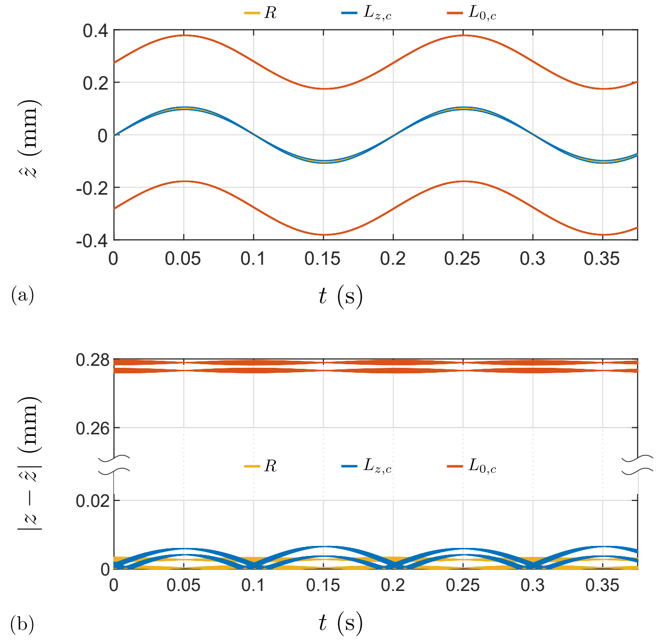

Fig. 9: Case study – Self-sensing technique robustness to $\pm 5\%$ errors on the machine impedance parameters. (a) Rotor axial estimate $\hat{z}$. (b) Estimation error.

errors on the machine parameters. The spin speed setpoint is set to 300 (rpm) and the sinusoidal position reference is still imposed. The load force and torque are fixed to 0.5 (N) and 50 (mNm). Figs. 9(a) and 9(b) depict the time evolution of the actual and estimated rotor displacement and the resulting position error respectively. An inaccuracy on the electrical resistance R has almost no effect on the position estimate given its limited impact on the winding impedance. As can be deduced from (10), the incorrect identification of the synchronous variational inductance coefficient $L_{z,c}$ only results in a scaling error, approximately equal to the parameter deviation, implying that the rotor can thus still be controlled in centred position. In contrast, as expected, a precise evaluation of the centred synchronous inductance coefficient $L_{0,c}$ is essential since the variation with the rotor displacement of the inductance is of the same order of magnitude as the error, leading to a significant offset on the axial position estimate. Note that the error considered in this study is substantial assuming that the inductance coefficients are measured during the commissioning phase of the machine.

V. Conclusion

This paper introduces, develops and validates an injection-based self-sensing technique allowing to estimate the rotor axial position of self-bearing motors. The electromechanical model predicting the rotor axial and spin dynamics of the machine under study is first derived, highlighting that the position information can be extracted from the winding synchronous inductance coefficient variation. The proposed self-sensing technique relies on the injection of a high frequency pulsating square-wave signal in the Park reference frame. Expressions linking the resulting high frequency current amplitude to the winding synchronous inductance coefficient as well as the latter to the rotor axial position are established in the general case and assuming that the electrical resistance is negligible.

In the framework of a case study, the self-sensing technique operation principle and tracking capabilities are validated on the basis of a specific sequence including position, spin speed and load variation. The simplified estimate is also shown to offer sufficient accuracy despite the low inductance coefficients due to the stator slotless structure. The robustness to errors on the machine impedance parameters is then investigated, underlining that a proper identification of the synchronous inductance coefficient in centred position is crucial to correctly estimate the rotor axial position whereas the remaining parameters only have a slight influence.

Future works comprise the experimental validation of the proposed injection-based self-sensing technique, including a state filter to mitigate the impact of current measurement noise, as well as the development of the transition scheme towards the observer-based technique implemented for high speed.

References

[1] J. Chen, J. Zhu, and E. L. Severson, "Review of bearingless motor technology for significant power applications," *IEEE Transactions on Industry Applications*, vol. 56, no. 2, pp. 1377–1388, 2020.

[2] J. Van Verdeghem, M. Lefebvre, V. Kluyskens, and B. Dehez, "Dynamical modeling of passively levitated electrodynamic thrust self-bearing

machines," *IEEE Transactions on Industry Applications*, vol. 55, no. 2, pp. 1447–1460, March 2019.

[3] G. C. Rubio and A. Chiba, "Design and analysis of a bearingless motor with passive axial suspension through null-flux coils," in *International Electric Machines & Drives Conference*, 2019, pp. 779–786.

[4] G. C. Rubio, Y. Fujii, and A. Chiba, "A bearingless motor with passive electrodynamic suspension in axial direction," *IEEE Transactions on Industry Applications*, vol. 57, no. 6, pp. 6812–6822, 2021.

[5] J. Van Verdeghem, A. Robert, S. Herrman, and B. Dehez, "Impact of ferromagnetic yokes on axial flux passively levitated self-bearing machines," in *2022 25th International Conference on Electrical Machines and Systems (ICEMS)*, 2022, pp. 1–6.

[6] J. Van Verdeghem, E. Severson, and B. Dehez, "Hybrid active-passive actuation approach of passively levitated thrust self-bearing machines," *IEEE Transactions on Industry Applications*, vol. 57, no. 6, pp. 7035–7045, 2021.

[7] G. C. Rubio, Y. Fujii, and A. Chiba, "Bearingless motor with asymmetric axial electrodynamic stabilization," in *Joint Technical Meeting on Magnetics/Motor Drive/Linear Drives*, 2021.

[8] N. Petersen, T. Slininger, and E. L. Severson, "State observers and run-out reduction for magnetically levitated motor systems," *IEEE Transactions on Industry Applications*, vol. 59, no. 2, pp. 1812–1823, 2023.

[9] Y. Hua and H. Zhu, "Rotor radial displacement sensorless control of bearingless permanent magnet synchronous motor based on mras and suspension force compensation," *ISA Transactions*, vol. 103, pp. 306–318, 2020.

[10] K. Li, F. Ling, X. Sun, Y. Cai, D. Zhao, and Z. Yang, "Displacement sensorless control for bearingless induction motor drives based on the mras method," *International Journal of Applied Electromagnetics and Mechanics*, vol. 62, pp. 787–805, 2020.

[11] H. Nian, Y. He, D. Chen, and L. Huang, "Self-sensing of the rotor position and displacement for an inset permanent magnet type bearingless motor," in *2007 International Conference on Electrical Machines and Systems (ICEMS)*, 2007, pp. 1508–1512.

[12] N. Petersen and E. L. Severson, "Suitability of bearingless motor windings for non-salient rotor displacement self-sensing," in *2022 IEEE Energy Conversion Congress and Exposition (ECCE)*, 2022, pp. 1–8.

[13] J. Van Verdeghem and B. Dehez, "Observer-based self-sensing techniques for hybrid active-passive self-bearing machines," in *18th Int. Symposium on Magnetic Bearings (ISMB)*, July 2023.

[14] J. Asama, T. Tai, and A. Chiba, "Development of axial-flux single-drive bearingless motor with one-axis active positioning," *IEEE Transactions on Industry Applications*, vol. 57, no. 6, pp. 6792–6800, 2021.